

This article was downloaded by:

On: 26 January 2011

Access details: *Access Details: Free Access*

Publisher *Taylor & Francis*

Informa Ltd Registered in England and Wales Registered Number: 1072954 Registered office: Mortimer House, 37-41 Mortimer Street, London W1T 3JH, UK



## Liquid Crystals

Publication details, including instructions for authors and subscription information:

<http://www.informaworld.com/smpp/title~content=t713926090>

### Electromechanical effect in cholesteric mixtures with a compensation temperature

H. P. Padmini<sup>a</sup>; N. V. Madhusudana<sup>a</sup>

<sup>a</sup> Raman Research Institute, Bangalore, India

**To cite this Article** Padmini, H. P. and Madhusudana, N. V.(1993) 'Electromechanical effect in cholesteric mixtures with a compensation temperature', *Liquid Crystals*, 14: 2, 497 – 511

**To link to this Article:** DOI: 10.1080/02678299308027665

**URL:** <http://dx.doi.org/10.1080/02678299308027665>

PLEASE SCROLL DOWN FOR ARTICLE

Full terms and conditions of use: <http://www.informaworld.com/terms-and-conditions-of-access.pdf>

This article may be used for research, teaching and private study purposes. Any substantial or systematic reproduction, re-distribution, re-selling, loan or sub-licensing, systematic supply or distribution in any form to anyone is expressly forbidden.

The publisher does not give any warranty express or implied or make any representation that the contents will be complete or accurate or up to date. The accuracy of any instructions, formulae and drug doses should be independently verified with primary sources. The publisher shall not be liable for any loss, actions, claims, proceedings, demand or costs or damages whatsoever or howsoever caused arising directly or indirectly in connection with or arising out of the use of this material.

## Electromechanical effect in cholesteric mixtures with a compensation temperature

by H. P. PADMINI and N. V. MADHUSUDANA\*

Raman Research Institute, Bangalore 560080, India

An electromechanical effect arises in cholesteric (N\*) liquid crystals due to a cross-coupling between fluxes and forces specific to chiral systems. We recently described an experiment to study this effect on samples with fixed boundary conditions. Here, we have derived the basic theoretical expressions relevant to this experiment. We have now used this technique to record the electromechanical signal across the compensation temperature of cholesteric mixtures consisting of cholesteryl chloride, 4'-heptyl-4-cyanobiphenyl and 2-cyano-4-heptylphenyl 4'-pentylbiphenyl-4-carboxylate. The sign of the electromechanical signal changes at the compensation point, clearly demonstrating the macroscopic origin of this effect.

### 1. Introduction

In cholesteric liquid crystals the molecular chirality results in a helical arrangement of the director with a temperature-dependent pitch ( $P$ ) which is usually of the order of a micrometer. This macroscopic chirality of the medium gives rise to some interesting cross-coupling terms between hydrodynamic fluxes and forces. One of the first physical experiments on liquid crystals by Lehmann [1] demonstrated such a cross-coupling effect. He found that cholesteric drops subjected to a vertical temperature gradient were set into continuous rotation. The hydrodynamic theory of cholesterics was developed in the late sixties by Leslie who obtained solutions corresponding to the Lehmann rotation phenomenon. Similar solutions were obtained later by Lubensky [2] and Martin *et al.* [3] in their developments of the hydrodynamic theory of cholesterics. The Lehmann rotation, due to thermomechanical coupling, requires that the anchoring energy for the azimuthal angle at the boundaries of the cholesteric drop must be zero. It is not easy to realize this condition experimentally. The analogous rotation phenomenon due to an electromechanical effect was described by Madhusudana and Pratibha in 1987 [4,5]. In order to get flat cholesteric drops with the required geometry, a very special combination of chemicals was used in that experiment.

It is very much easier to realise strong anchoring of the nematic director at appropriately treated glass plates. We described earlier [6] an experiment in which the electromechanical effect was demonstrated in a sample with such fixed boundary conditions. The director of the cholesteric is fixed parallel to the bounding surfaces of the cell. An electric field applied across the cell produces a non-uniform distortion of the profile of azimuthal angles due to the electromechanical effect. The non-uniform distortion changes sign with that of the electric field. This type of pure azimuthal distortion can be expected to occur in materials with negative dielectric anisotropy (assuming that we are not above the threshold for an electrohydrodynamic instability). However, since the birefringence of the liquid crystal materials is usually large and the

\* Author for correspondence.

distortion angle is much less than the optical phase difference produced by the cell, the Mauguin criterion applies and the distortion cannot be detected optically. In order to overcome this problem, we used materials with weak positive dielectric anisotropy in our experiment [6]. The director field develops a tilt distortion above the Fréedericksz threshold in such a case. If the tilt angle is sufficiently large, the effective birefringence and hence the phase difference produced by the cell decreases. The electro-optic signal due to the electromechanical distortion of the azimuthal profile becomes detectable in such a case. As the electromechanical distortion is linear in the applied electric field  $E$ , the corresponding optical signal is produced at the frequency of the applied AC field. On the other hand, the dielectric distortion depends quadratically on the applied field and the corresponding time-dependent optical signal has twice the frequency of the AC field. The distortion in the azimuthal profile produces an optical signal which is maximized when the director orientation at the boundary is set at an angle of  $\pi/8$  radians with respect to the polarizer. On the other hand, the tilt angle variations produce a signal which is maximized for a setting at  $\pi/4$  radians [6]. Indeed our experiments clearly showed that the  $f$  signal due to the electromechanical coupling had maxima at  $\pi/8$  and  $3\pi/8$  radians while the  $2f$  signal due to the dielectric coupling had a maximum at  $\pi/4$  radians.

In hydrodynamic theories, the electromechanical coupling coefficient ( $v_E$ ) is related to the macroscopic chirality of the system. Indeed  $v_E$  is expected to change sign with that of the helix [7]. This was confirmed in the earlier experiments on the cholesteric drops. By doping the liquid crystal with different chiral compounds we could obtain cholesterics with opposite handedness. The sense of rotation was indeed found to reverse with that of the handedness of the helical arrangement [5]. Further, using a mixture in which two chiral materials producing opposite handedness were mixed in a proportion to obtain an infinite pitch, the drops did not rotate under an applied field [6]. While these observations clearly demonstrate that the electromechanical coupling coefficient depends largely on the macroscopic chirality, it is possible that the molecular chirality can have a non-zero contribution. In fact an earlier experiment by Eber and Janossy [8, 9] was based on this assumption. They set-up an experiment to measure the thermomechanical coefficient of a mixture whose composition and temperature were adjusted to be close to the compensation temperature. We however note that there has been some discussion in the literature on the interpretation of this experiment [10, 11]. Indeed hydrodynamic theories predict that the cross-coupling term should be proportional to  $Q(=2\pi/P)$ , the wavevector of the helix. In a compensated cholesteric, the helical pitch increases as the temperature is lowered towards a compensation temperature ( $T_c$ ) at which  $P$  becomes infinite. As the temperature is lowered further the handedness of the helix reverses and the pitch again decreases. The wavevector close to  $T_c$  varies linearly with temperature, becoming 0 at  $T_c$ .

Since we have developed a technique of detecting the electromechanical signal using samples with fixed boundary conditions, we thought it worthwhile to study a compensated cholesteric mixture across  $T_c$ . We report here our experimental observations, which essentially confirm the predictions of hydrodynamic theories. In the next section we give the theoretical background to the experimental technique.

## 2. Theoretical background

We consider a cholesteric liquid crystal with a natural helical wavevector  $Q_0$  taken between two conducting glass plates separated by a gap  $D$  (see figure 1). The lower plate

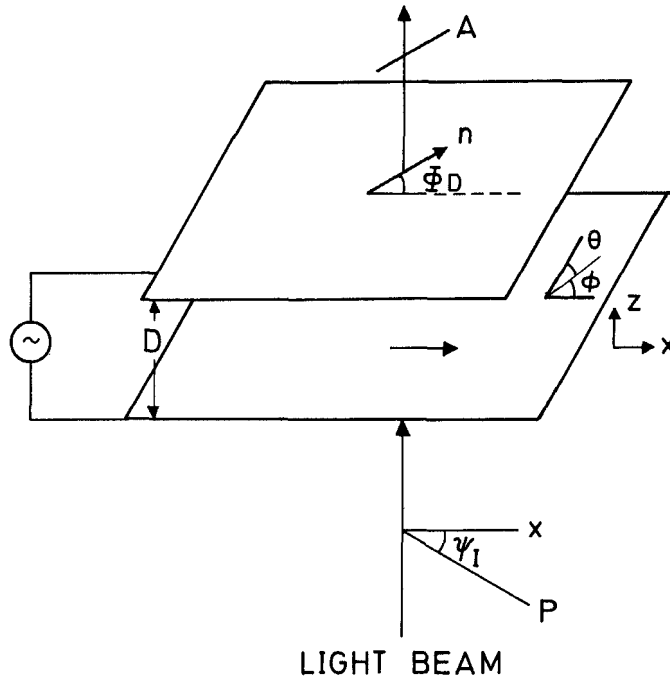


Figure 1. Schematic diagram of the experimental geometry. P and A are the polarizer and analyser respectively.

is treated for an alignment of the director in the plane of the plate along the  $X$ -axis. The upper plate is treated for an alignment along a direction making an azimuthal angle  $\phi_D$  with respect to the  $X$ -axis. The material has a dielectric anisotropy  $\Delta\epsilon = \epsilon_{\parallel} - \epsilon_{\perp}$ , where  $\epsilon_{\parallel}$  is the dielectric constant in a direction parallel to the director  $\mathbf{n}$  and  $\epsilon_{\perp}$  that perpendicular to  $\mathbf{n}$ . (We ignore the small biaxiality of the cholesteric medium.) We assume that  $\Delta\epsilon > 0$ . When we apply an AC electric field at a frequency  $f$  between the two tin oxide coated plates, the azimuthal profile becomes non-uniform and oscillates at the frequency  $f$  because of the electromechanical coupling coefficient  $\nu_E$  [6]. In the present geometry, there is no contribution to the orientation of the director from the other independent electromechanical coefficient [7]. Since the electromechanical effect is linear in  $E$ , there is no threshold for this distortion. As we discussed in the introduction, this distortion is not detectable optically in view of the strong anchoring conditions at the two boundaries. As the applied field is increased beyond the Fréedericksz threshold value, the director field also develops a tilt distortion. The components of the director in the  $XYZ$  coordinate system (figure 1) are

$$\mathbf{n} \equiv (\cos \theta \cos \phi, \cos \theta \sin \phi, \sin \theta). \quad (1)$$

Beyond the Fréedericksz threshold, both  $\theta$  and  $\phi$  are functions of the  $z$ -coordinate. The elastic energy density of the distorted medium is given by

$$F_d = \frac{k_{11}}{2} (\text{div } \mathbf{n})^2 + \frac{k_{22}}{2} (\mathbf{n} \cdot \text{curl } \mathbf{n} - Q_0)^2 + \frac{k_{33}}{2} (\mathbf{n} \times \text{curl } \mathbf{n})^2, \quad (2)$$

where  $k_{11}$ ,  $k_{22}$  and  $k_{33}$  are the splay, twist and bend elastic constants, respectively. The dielectric energy density is

$$F_{\text{diel}} = -\frac{\Delta\epsilon}{8\pi} (\mathbf{n} \cdot \mathbf{E})^2. \quad (3)$$

The field is applied along the  $z$ -direction, i.e.  $E = E_z$ . For the sake of simplicity, we assume that the medium is free from ionic impurities, i.e.

$$\operatorname{div} D = 0. \quad (4)$$

Since variations occur only along the  $z$ -direction, this means that  $\partial D_z / \partial z = 0$  or  $D_z = \text{constant}$ , where

$$D_z = \varepsilon_{\perp} E_z + \Delta \varepsilon n_z^2 E_z, \quad (5)$$

which gives

$$E_z = \frac{D_z}{(\varepsilon_{\perp} + \Delta \varepsilon n_z^2)}. \quad (6)$$

The voltage applied across the sample is

$$V = \int_0^D E_z dz = D_z \int_0^D \frac{dz}{(\varepsilon_{\perp} + \Delta \varepsilon n_z^2)}. \quad (7)$$

We ignore a small flexoelectric contribution to the free energy density arising from the non-uniform field  $E_z$ . Our earlier experiments [6] have shown that the  $f$  signal arises due to  $\phi$  oscillations and not  $\theta$  oscillations. This means that the flexoelectric contribution to the distortion is negligible.

The molecular field [7] corresponding to the elastic and dielectric energy densities is obtained by using the relation

$$\mathbf{h}_{\alpha} = -\frac{\partial F}{\partial n_{\alpha}} + \frac{\partial}{\partial z} \left[ \frac{dF}{d(\partial n_{\alpha} / \partial z)} \right]. \quad (8)$$

The electromechanical contribution to the molecular field for the present geometry is given [7] by

$$h^{\text{EM}} = \nu_E \mathbf{n} \times \mathbf{E}. \quad (9)$$

In considering the hydrodynamic contribution, for the sake of simplicity, we ignore all velocities and take into account only the rotational motion of the director. We then get

$$h_{\alpha}^{\text{hydro}} = \gamma_1 \dot{n}_{\alpha}, \quad (10)$$

where the dot represents the time derivative and  $\gamma_1$  is the rotational viscosity constant [7]. We can now write the torque balance relations taking into account the molecular fields due to all the processes listed above, i.e. with  $\Gamma = \mathbf{n} \times \mathbf{h}$

$$\Gamma^{\text{elastic}} + \Gamma^{\text{dielectric}} + \Gamma^{\text{EM}} = \Gamma^{\text{hydro}}. \quad (11)$$

There are only two independent torque balance relations for the director. Following the argument given by Bodenshatz *et al.* [12], we write the two independent components of the torque as follows:

$$\Gamma_2 = \sin \theta (h_x \cos \phi + h_y \sin \phi) - h_z \cos \theta, \quad (12)$$

and

$$\Gamma_3 = -h_x \sin \phi + h_y \cos \phi. \quad (13)$$

Using the earlier derivation of the molecular field components, and the components of the director given in equation (1), after some simplification we get

$$\begin{aligned} \Gamma_2 = & (k_{11} - k_{33}) \sin \theta \cos \theta \left( \frac{\partial \theta}{\partial z} \right)^2 \\ & + \{k_{33}(\cos 2\theta) - 2k_{22} \cos^2 \theta\} \sin \theta \cos \theta \left( \frac{\partial \phi}{\partial z} \right)^2 \\ & - (k_{11} \cos^2 \theta + k_{33} \sin^2 \theta) \frac{\partial^2 \theta}{\partial z^2} - 2Q_0 k_{22} \sin \theta \cos \theta \frac{\partial \phi}{\partial z} \\ & - \frac{\Delta \varepsilon}{4\pi} \frac{D_z^2 \sin \theta \cos \theta}{(\varepsilon_{\perp} + \Delta \varepsilon \sin^2 \theta)^2} + \gamma_1 \dot{\theta} = 0, \end{aligned} \tag{14}$$

and

$$\begin{aligned} \Gamma_3 = & (k_{33} \sin^2 \theta + k_{22} \cos^2 \theta) \cos \theta \left( \frac{\partial^2 \phi}{\partial z^2} \right) \\ & + 2(k_{33} \cos 2\theta - 2k_{22} \cos^2 \theta) \sin \theta \left( \frac{\partial \theta}{\partial z} \right) \left( \frac{\partial \phi}{\partial z} \right) \\ & - 2k_{22} Q_0 \sin \theta \frac{\partial \theta}{\partial z} - \frac{v_E D_z \cos \theta}{(\varepsilon_{\perp} + \Delta \varepsilon \sin^2 \theta)} - \gamma_1 \cos \theta (\dot{\phi}) = 0. \end{aligned} \tag{15}$$

The above relations reduce in the static limit to those derived by Leslie [13] when  $v_E = 0$ . If an AC field at a frequency  $f$  is applied to the cell, we may write

$$D_z = D_{z0} \sin 2\pi f t. \tag{16}$$

The above equations have to be solved to obtain  $\theta(z, t)$  and  $\phi(z, t)$  to satisfy the boundary conditions

$$\theta(0, t) = \phi(0, t) = \theta(D, t) = \phi(D, t) = 0. \tag{17}$$

Equations (14) and (15) are coupled non-linear partial differential equations in  $\theta$  and  $\phi$ . If the material had negative dielectric anisotropy,  $\theta$  would be zero and the equations would reduce to those that we have already discussed in our earlier paper [6]. Note that since  $\theta \neq 0$  in the present problem,  $\theta$  and  $\phi$  get strongly coupled though the  $Q_0$ -dependent terms in equations (14) and (15). We have tried to solve these equations using the DPDES subroutine of the IMSL library. We found that the program was not very efficient for this purpose and required a very long computation time. In fact, we could only make calculations by dividing the thickness of the sample and the time period of the applied AC signal into only 15 equal parts. We have used the following material parameters in our calculations

$$\begin{aligned} k_{11} = 1.4 \times 10^{-11} \text{ N}, \quad k_{33} = 3 \times 10^{-11} \text{ N}, \quad \gamma_1 = 0.07 \text{ N s m}^{-2}, \\ \varepsilon_{\perp} = 4, \quad \Delta \varepsilon = 0.5, \quad \text{and} \quad v_E = 2Q_0 \times 10^{-5} [5]. \end{aligned}$$

The wavevector of the helix was assumed to be  $Q_0 = 0.4 \times 10^6 \text{ m}^{-1}$ . The sample thickness used,  $D = 3 \mu\text{m}$ , was a typical value used in the experiments. For an applied voltage of 6.4 V, we give illustrative  $z$ -profiles of  $\phi$  and  $\theta$  at three different times within the period  $T$  in figures 2 and 3 respectively. It is seen that  $\theta$  and  $\phi$  oscillations are out of

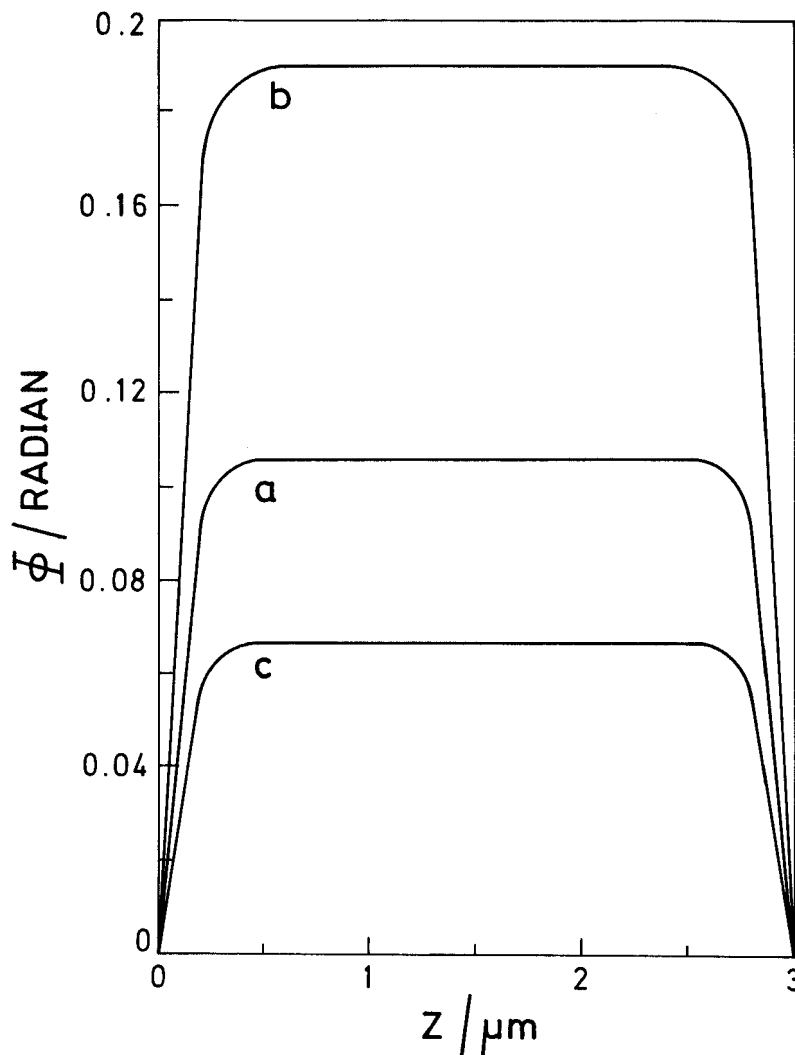


Figure 2. Numerically calculated  $z$ -dependence of the azimuthal angle  $\phi$  at three different times; (a) at  $t=0.267$  T, (b) at  $t=0.533$  T, and (c) at  $t=0.8$  T.

phase in relation to each other. Moreover, at 6.4 V, the  $\phi$  profile is practically flat, and the curvature in  $\phi$  occurs only near the two walls. This is probably connected with the fact that  $\theta$  takes a maximum value in the centre of the cell. The electromechanical coupling will become less effective as  $\theta$  increases, as the corresponding torque is  $\propto \cos \theta$ , see equation (15). We are now exploring ways of improving our calculations.

### 3. Experimental results and discussion

Our interest in the present paper is to study the temperature variation of the electromechanical effect across the compensation temperature ( $T_c$ ). We have used the following mixture which has a convenient compensation temperature and positive dielectric anisotropy as required in the experiment: 35.6 mol% of 2-cyano-4-heptylphenyl 4'-pentylbiphenyl-4-carboxylate [7P(2CN)5BC], 6.5 mol% of 4'-heptyl-

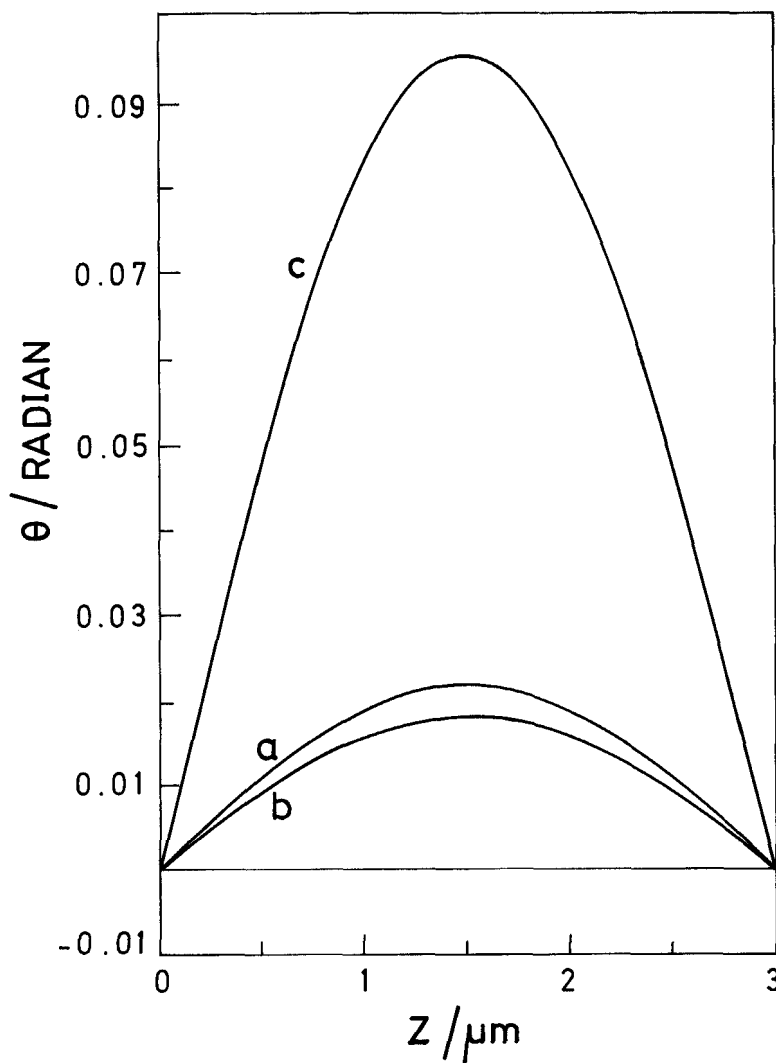


Figure 3. Numerically calculated  $z$ -dependence of the tilt angle  $\theta$  at three different times; (a) at  $t=0.267$  T, (b) at  $t=0.533$  T and (c) at  $t=0.8$  T.

4-cyanobiphenyl (7CB) and 57.9 mol% of cholesteryl chloride. We measured the pitch of the helix as a function of temperature using the Cano wedge technique [14]. A Mettler FP82 hot stage was used to control the temperature. The measurements were made using a Leitz polarizing microscope (Model Ortholux II POL-BK). The results on two mixtures with slightly different compositions are shown in figures 4 and 5. When  $T_c$  is far away from the cholesteric–isotropic transition point,  $Q_0$  varies practically linearly with temperature (see figure 4). We could not measure pitch values larger than  $\sim 35 \mu\text{m}$  using the wedge technique. However, we can clearly see from figures 4 and 5 that the wavevector follows a smooth curve passing through 0 at  $T_c$ . When we use monochromatic sodium light to illuminate the sample kept between crossed polarizers, dark bands parallel to the disclination lines can be seen. The relative motion of the dark bands, in relation to the edge of the wedge, as the analyser is rotated can be used to



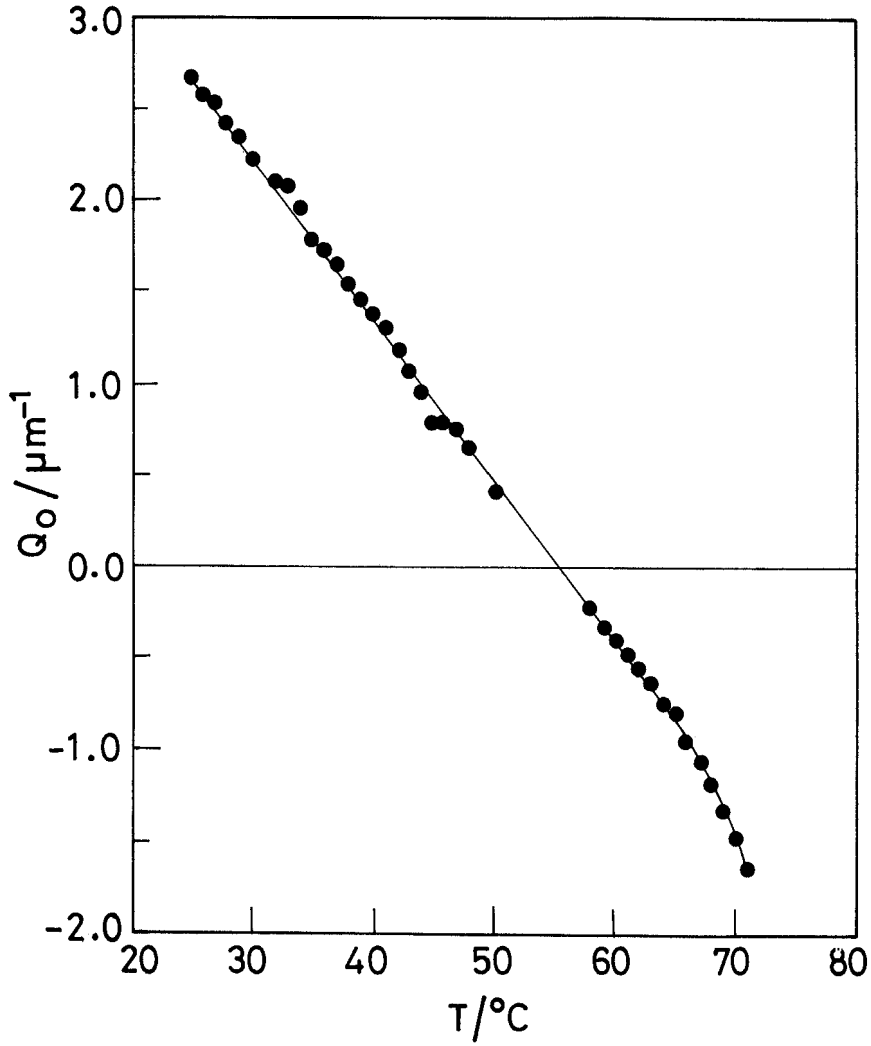


Figure 4. Temperature variation of the wavevector  $Q_0$  in a compensated cholesteric mixture.  $T_c$  is about  $15^\circ$  below the cholesteric–isotropic transition temperature.

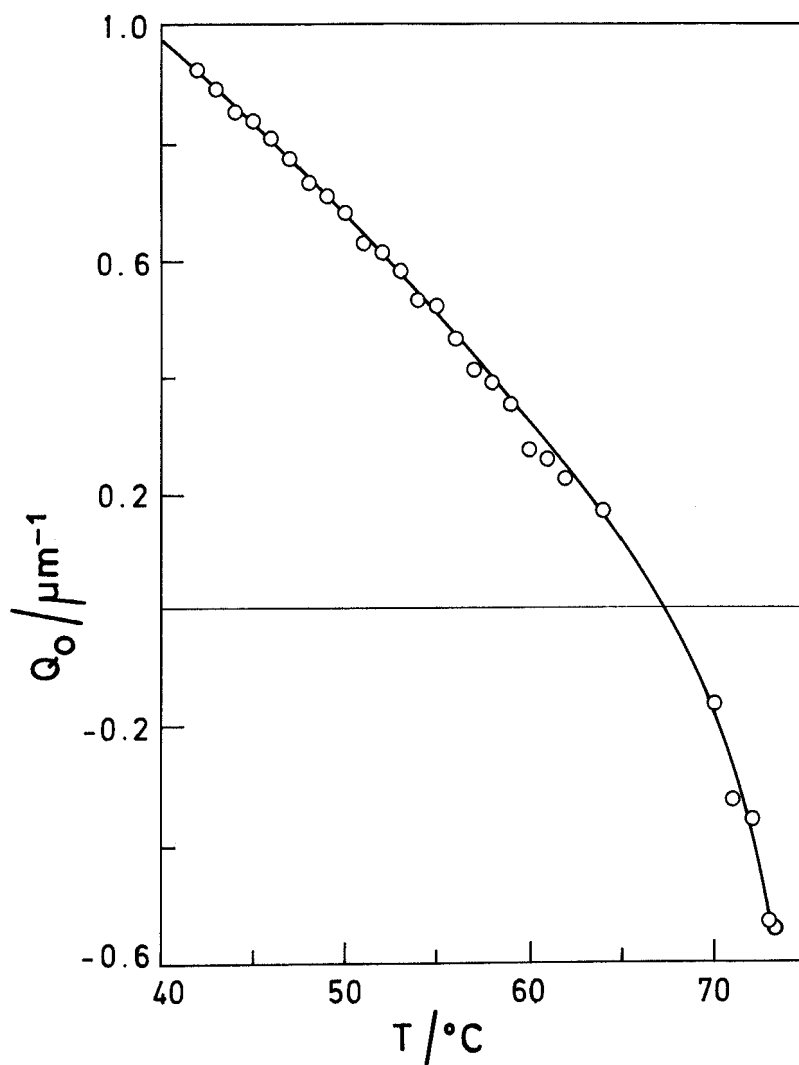


Figure 5. Temperature variation of the wavevector  $Q_0$  in a compensated cholesteric mixture in which  $T_c$  is only  $\sim 7^\circ$  below the cholesteric-isotropic transition point, resulting in a rapid variation of  $Q_0$  above  $T_c$ .

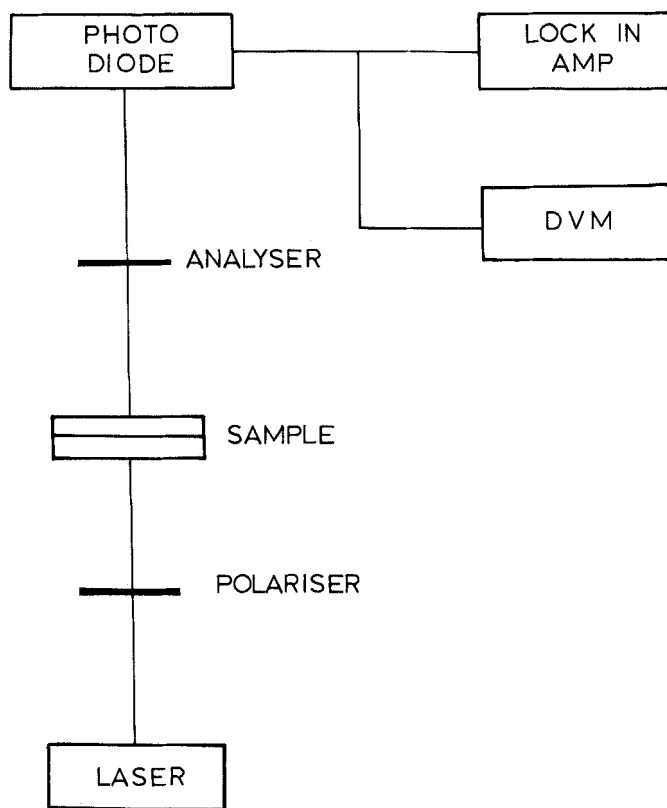


Figure 6. Block diagram of the experimental set-up used to measure the electro-optic signals.

determine the sense of the cholesteric helix. Using this technique, we have found that the helix is left handed at temperatures lower than  $T_c$  and right handed above  $T_c$ . When  $T_c$  is closer to the cholesteric–isotropic transition point, the wavevector increases rapidly close to the latter (see figure 5). The sample used in the electromechanical experiment is mounted between two ITO coated transparent conductors. The glass plates are pre-treated with a polyimide coating and unidirectionally rubbed to get homogeneous alignment of the director. The typical sample thickness is  $3\ \mu\text{m}$  which was fixed by using spacer beads. The block diagram of the experimental set-up is shown in figure 6. The sample mounted in a Mettler hot stage is kept on the stage of a Leitz polarizing microscope and aligned such that the rubbing direction makes an angle of  $\pi/8$  radians with the polarizer. The sample is illuminated with monochromatic radiation from a 1 mW helium–neon laser, and the light beam transmitted through an analyser, crossed with reference to the polarizer, is allowed to fall on a photodiode. The preamplified photodiode signal is connected both to a DC nanovoltmeter (Keithley Model 181) and to a PAR lock-in-amplifier (Model 5301A) to measure both the DC and AC outputs.

The sample was slowly cooled from the isotropic phase (at  $\sim 1^\circ/\text{min}$ ) to the cholesteric phase. As the pitch rapidly varies with temperature, usually a number of disclination lines separating regions of different pitch are seen in the field of view, the lines presumably originating near the edge of the sample. On rare occasions, we found a

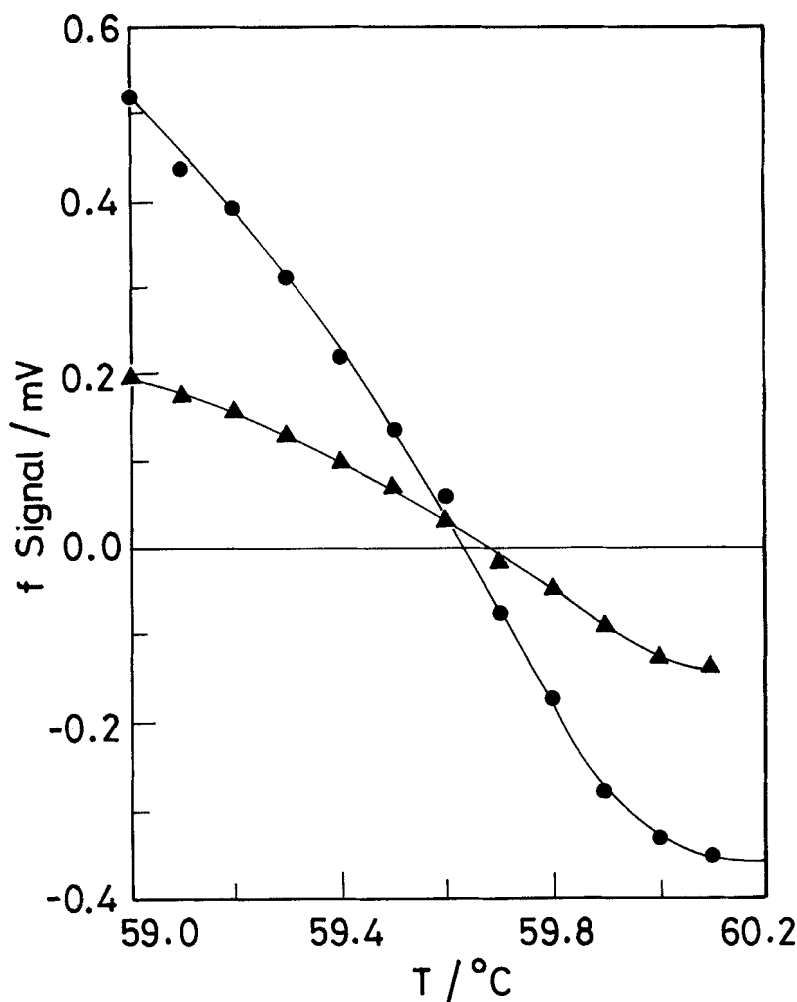


Figure 7. Temperature variations of the  $f$  signals at 17 Hz (●) and 37 Hz (▲). The small difference in  $T_c$  probably arises from a more efficient ionic heating at 17 Hz.

large enough area free of such disclinations which could be used for the electromechanical experiment. The sample thickness has to be quite small ( $\approx 3 \mu\text{m}$ ) to avoid the occurrence of striped domains on application of the electric field [15, 16] above a threshold value. As we discussed earlier, we can get the electromechanical signal at  $f$  only when the applied voltage is above the Fréedericksz threshold. The voltage cannot be too high either, since the electromechanical coupling becomes less effective as the tilt angle of the director increases. In our material, the RMS value of the Fréedericksz threshold was  $\approx 1.2 \text{ V}$ , and we found it convenient to record the electromechanical signal at an RMS voltage =  $2.8 \text{ V}$ . Measurements were made at a few different frequencies of the applied sinusoidal electric field. The  $f$  and  $2f$  signals were recorded along with their phases as the temperature was lowered across the compensation temperature. At each temperature, measurements were made at different frequencies before the temperature was lowered. A preliminary run at two frequencies (17 and 37 Hz) is shown in figure 7. As the temperature approaches  $T_c$ , the magnitude of the  $f$

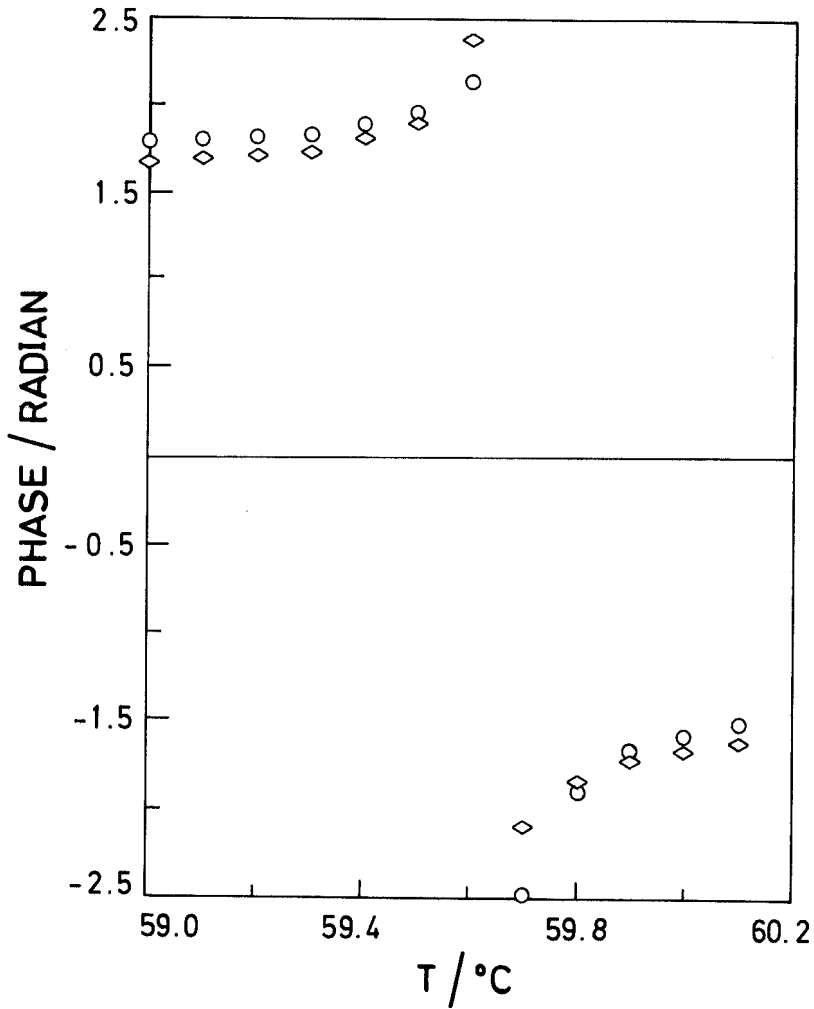


Figure 8. Temperature variations of the phase angle of the  $f$  signal at 17 Hz (◇) and 37 Hz (○). Note the change of sign of the phase angle at  $T_c$ .

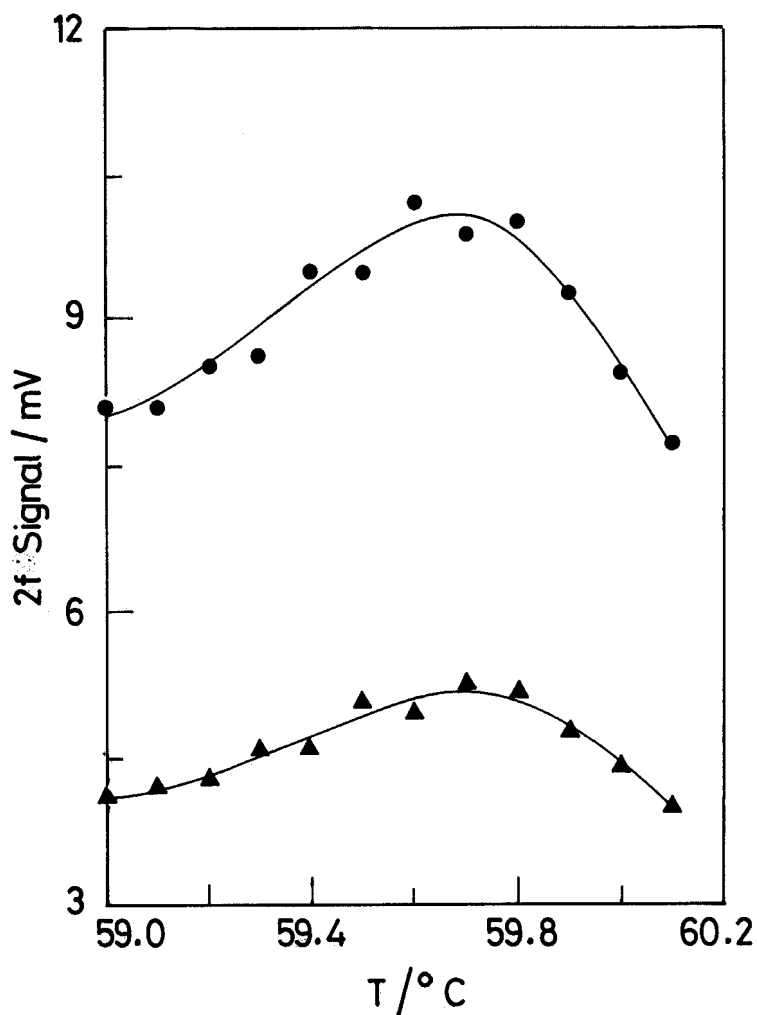


Figure 9. Temperature variations of the  $2f$  signals at 17 Hz (●) and 37 Hz (▲). Note the peak in the signal close to  $T_c$ .

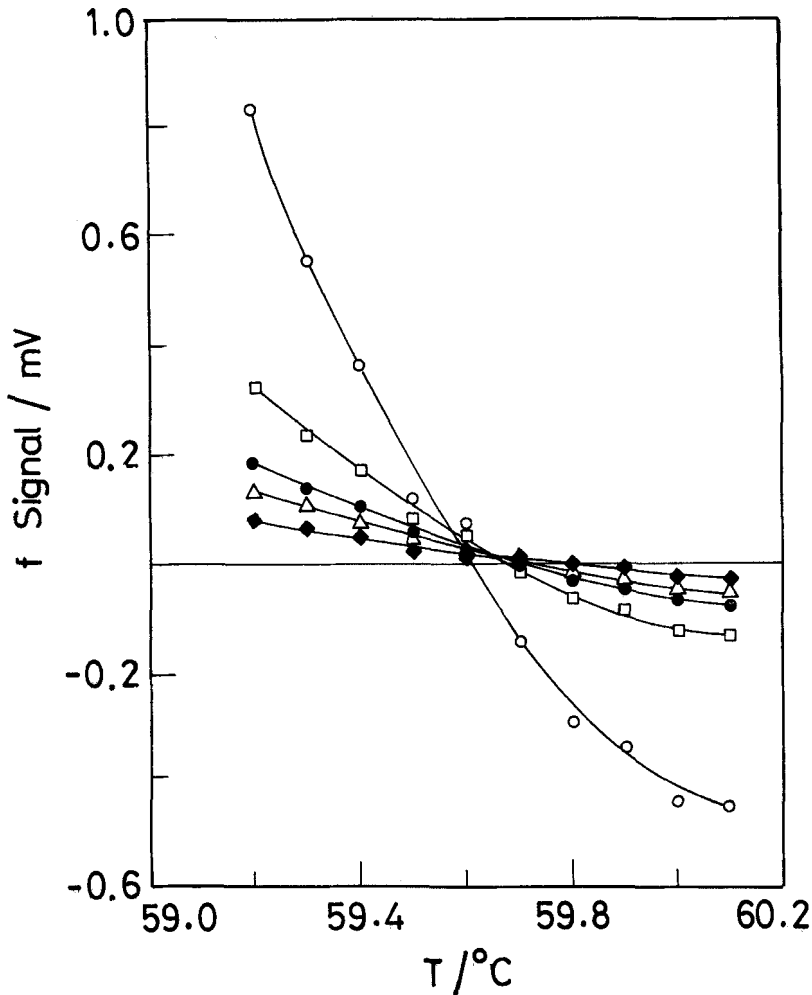


Figure 10. Temperature variations of the  $f$  signal at 7 Hz (○), 17 Hz (□), 27 Hz (●), 37 Hz (△) and 57 Hz (◆).

signal decreases. The phase angle of the signal also increases. As we cross  $T_c$ , the signal again grows but with the opposite phase angle (figure 8). The phase angle decreases in magnitude as the temperature is further lowered. The signal amplitude itself grows. The result clearly shows that the electromechanical coupling coefficient goes to zero and changes sign as we cross  $T_c$ . We also note that the signal at 17 Hz goes to zero at a slightly lower temperature ( $\sim 0.05^\circ$ ) compared to the signal at 37 Hz. This arises probably because of greater ion flow at the lower frequency and the consequent additional heating of the sample, thus altering its true temperature from the measured value.

The amplitudes of the  $2f$  signals are shown in figure 9 for 17 and 37 Hz. Interestingly, the signal shows a maximum at  $T_c$  in both cases, while the phase angle is practically independent of temperature. We believe that the origin of this maximum is due to the absence of twist distortions in the sample with  $Q_0 = 0$ , i.e. at  $T_c$ . When  $Q_0 \neq 0$  and the sample has a twist distortion, the effective Fréedericksz threshold is somewhat

higher than when  $Q_0=0$ . Thus, at the constant applied voltage of 2.8 V, the  $\theta$ -oscillations due to the dielectric coupling have a somewhat higher amplitude for  $Q_0=0$  as the threshold is lower. Some preliminary experiments indicate that the threshold voltage is  $\sim 0.07$  V lower close to  $T_c$  compared to the value at  $\sim T_c + 0.5^\circ$ .

More detailed measurements at 5 different frequencies lying between 7 and 57 Hz are shown in figure 10. These readings were taken as the sample was heated across  $T_c$ . The cross-over of the electromechanical signal as the temperature is varied across  $T_c$  is again clear. Understandably, as the frequency is increased, the amplitude of the signal is lowered. The variation of the signal is linear close to  $T_c$ . The slope of the signal versus temperature curve is approximately inversely proportional to the frequency (to  $\sim \pm 20$  per cent). We also note that as the temperature is increased, the electromechanical signal tends to vary more slowly. We can only guess that this may be caused by variation of all the material parameters like the elastic constants,  $\Delta\epsilon$ , etc., with temperature.

Thus our experimental results again bring out clearly the dependence of the electromechanical coupling coefficient on the macroscopic chirality of the cholesteric medium.

### References

- [1] LEHMANN, O., 1900, *Annln Phys.*, **2**, 649.
- [2] LUBENSKY, T. C., 1972, *Phys. Rev. A*, **6**, 452.
- [3] MARTIN, P. C., PARODI, P., and PERSHAN, P. J., 1972, *Phys. Rev. A*, **6**, 2401.
- [4] MADHUSUDANA, N. V., and PRATIBHA, R., 1987, *Molec. Crystals liq. Crystals*, **5**, 43.
- [5] MADHUSUDANA, N. V., and PRATIBHA, R., 1989, *Liq. Crystals*, **5**, 1827.
- [6] MADHUSUDANA, N. V., PRATIBHA, R., and PADMINI, H. P., 1991, *Molec. Crystals liq. Crystals*, **202**, 35.
- [7] DE GENNES, P. G., 1974, *The Physics of Liquid Crystals* (Clarendon).
- [8] EBER, N., and JANOSSY, I., 1982, *Molec. Crystals liq. Crystals*, **72**, 233.
- [9] EBER, N., and JANOSSY, I., 1984, *Molec. Crystals liq. Crystals Lett.*, **102**, 311.
- [10] PLEINER, H., and BRAND, H. R., 1987, *Molec. Crystals liq. Crystals Lett.*, **5**, 61.
- [11] PLEINER, H., and BRAND, H. R., 1988, *Molec. Crystals liq. Crystals Lett.*, **5**, 183.
- [12] BODENSCHATZ, E., ZIMMERMANN, W., and KRAMER, L., 1988, *J. Phys., Paris*, **49**, 1875.
- [13] LESLIE, F. M., 1970, *Molec. Crystals liq. Crystals*, **12**, 57.
- [14] CANO, R., and CHATELAIN, P., 1961, *C. r. hebd. Séanc. Acad. Sci., Paris*, **253**, 2081.
- [15] CHIGRINOV, V. G., BELYAEV, V. V., BELYAEV, S. V., and GREBENKIN, M. F., 1979, *Sov. Phys. JETP*, **50**, 994.
- [16] COHEN, G., and HORNREICH, R. M., 1990, *Phys. Rev. A*, **41**, 4402.